encit 2020

ABCM Associação Brasileira de Engenharia e Ciências Mecânicas

18th Brazilian Congress of Thermal Sciences and Engineering
November 16-20, 2020 (Online)

ENC-2020-0425
FREEZE-CASTING METHOD AS AN ALTERNATIVE FOR CERAMIC CAPILLARY EVAPORATOR MANUFACTURING

Marcos Vinício Oro
Frederico Marques Baumgratz
Caio Dias Fernandes
Edson Bazzo
Federal University of Santa Catarina, Department of Mechanical Engineering
LabCET - Laboratory of Combustion and Thermal Systems Engineering, 88040-900. Florianópolis / SC, Brazil
oro@labcet.ufsc.br; fredbaumgratz@gmail.com; caio.diasfernandes@gmail.com; e.bazzo@ufsc.br

Isadora Schramm Deschamps
Marcio Celso Fredel
Federal University of Santa Catarina, Department of Mechanical Engineering
CERMAT - Ceramic & Composite Materials Research Laboratories, 88040-900. Florianópolis/SC, Brazil
isadora.deschamps@labmat.ufsc.br; m.fredel@ufsc.br

Abstract. *Ceramic capillary evaporators have been proposed as an alternative to integrate two-phase passive thermal control systems. In the present work, the freeze casting method is considered for porous structures manufacturing and subsequent integration in a capillary pumped loop (CPL). Different sets of alumina samples were manufactured and characterized to obtain porosity, capillary pressure, critical diameter and permeability. Deionized water was used as the working fluid for the CPL thermal performance experiment. Throughout sample characterization the following results were found: porosity from 69 to 84 %, permeability from* $1x10^{-12}$ *to* $6\ x10^{-12}$ *m², critical diameter from 11 to 40 µm and capillary pumping pressure from 7 to 26 kPa. The thermal performance of three samples was evaluated on a CPL, which was able to operate stably with application of powers in the evaporator up to 44 W (7 W/cm²), corresponding to a total thermal resistance of about 3 K/W (16 cm²·K/W). Although further investigations are necessary, the freeze casting method proved to be successful and valid for the manufacture of ceramic capillary evaporators.*

Keywords: *freeze casting, capillary pumped loop, ceramic evaporator, alumina*

1. INTRODUCTION

The thermal control of electronic equipment has been widely studied to ensure their operation and performance. Passive two-phase devices such as heat pipes, capillary pumped loops (CPL) and loop heat pipes (LHP) have successfully been used as a cooling system for electronic equipment, especially in microgravity environments. In general, the performance of the cooling system is controlled mainly by the capillary structure's features. In this work, the use of a CPL was considered to evaluate the performance of the proposed porous structure. It should be noted such porous structure could also be adapted to integrate other two-phase cooling systems.

The CPL consists of a capillary evaporator, a condenser, a reservoir, a liquid line and a vapor line, as shown in Fig. 1. The CPL cooling device operation is based on the evaporation of a working fluid (water, ammonia, acetone, etc.) from a heat source, which is supplied to the evaporator (for example from an electrical equipment) and the vapor flows to a condenser through the line, and then, heat is removed from the condenser and the fluid returns to the liquid state. Finally, the liquid flows to the evaporator by capillary action to complete the loop. The reservoir is used to stabilize the system, controlling the operating temperature.

In general, a large number of material types have been considered for manufacturing the capillary structure, among which are highlighted nickel and stainless steel (Reimbrecht et al., 2003), cooper (Maydanik, 2005), polyethylene (Camargo, 2004; Cerza et al., 2001) and ceramic material based on alumina (Baumgratz et al., 2017; Berti et al., 2011; Camargo, 2004; Deschamps et al., 2015; Santos et al., 2012).

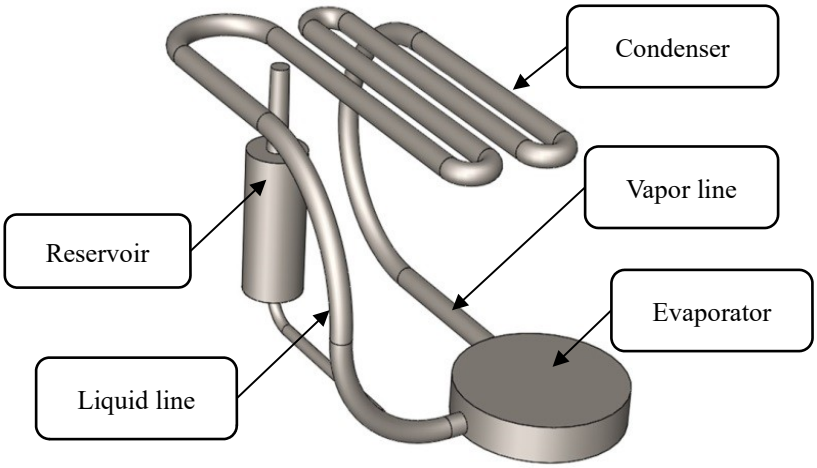

Figure 1. Capillary pumped loop representation.

In recent years, some alternatives have been proposed to replace conventional capillary evaporators. Maydanik et al. (2014) report that with a biporous capillary structure makes it possible to increase the thickness of the evaporating layer and to reduce the pressure losses. As a result a considerable decrease in the evaporator thermal resistance can be achieved. Semenic and Catton (2009) show the better performance of biporous wicks compared to monoporous wicks. Guo et al. (2020a) report that in a biporous wick the small pores can provide large capillary pressure, while the large pores reduce flow resistance, therefore, from the perspective of flow, two different sizes pores can solve the contradiction of capillary force and flow resistance.

Recently, Guo et al. (2020b) manufactured a LHP with a superhydrophilic porous wick, which was made by copper powder sintering and surface modification through hydrogen peroxide (H_2O_2) oxidation. The heat transfer performance was significantly enhanced in comparison with a conventional porous wick. The authors highlight three aspects: large capillary force, multi-scale structures in the nanometer to millimeter range, and more nucleation sites and a large surface area for phase change heat transfer.

Putra et al. (2014) proposed the use of biomaterial as a wick. They tested four types of corals and compared with some cooper sintered power wicks in a LHP device. The results showed that the thermal resistance was reduced by approximately 56 % with the use of the biomaterial tabulate wick instead of sintered copper power wick. In a subsequent search, Putra and Septiadi (2017) integrated a coral biomaterial (tabulate) wick in a heat pipe. The results showed better performance when compared to a sintered copper powder wick heat pipe. Recently, Solomon et al. (2020) assessed a natural bio-carbon based wick structure on the performance of a compact LHP. The carbon material for the wick structure was prepared by carbonizing the Karuvelam wood. The results presented similar performances compared with conventional wicked compact LHPs, but with the advantages such as lightweight, high capillarity, availability, and environmentally safe nature.

Another alternative was proposed by Kumar and Arakeri (2020): a porous media consisting of closely packed capillaries. Capillary tubes are kept in contact allowing a bulk meniscus to occur between the external surfaces. The internal volume of each capillary tube operates as a fluid reservoir, which feeds the bulk meniscus. The technology was not implemented in thermal control systems and further studies are needed to prove the applicability of the proposed system.

Hu et al. (2020) adopted a 3D printing technology to design and manufacture the capillary wicks of LHPs using 316 stainless steel powder. The authors claim that through this technique it was possible to control the structural parameters so that the optimum wick with high porosity, suitable pore radius, high permeability and low effective thermal conductivity could be realized. However, the manufacturing process appears to be expensive and time-consuming.

Initial studies presented by Baumgratz et al. (2017) suggest that the freeze casting method can provide ceramic structures with suitable features for use in capillary evaporators.

The freeze casting process involves the controlled freezing of a liquid with suspended ceramic particles (i.e.: a ceramic slurry), in such a manner as to form vertically ordered ice crystal lamellae. As the freezing front advances the suspended ceramic particles are trapped outside the newly-formed ice crystals. The frozen structure is then lyophilized, sublimating the ice lamellae and creating a vertically ordered porous structure, which - once properly sintered - constitutes the ceramic capillary evaporator. A schematic overview of the process is illustrated in Fig. 2. This work aims at showing the technical feasibility of using freeze casting for the production of ceramic structures capable of integrating heat transfer systems consisting of capillary evaporators.

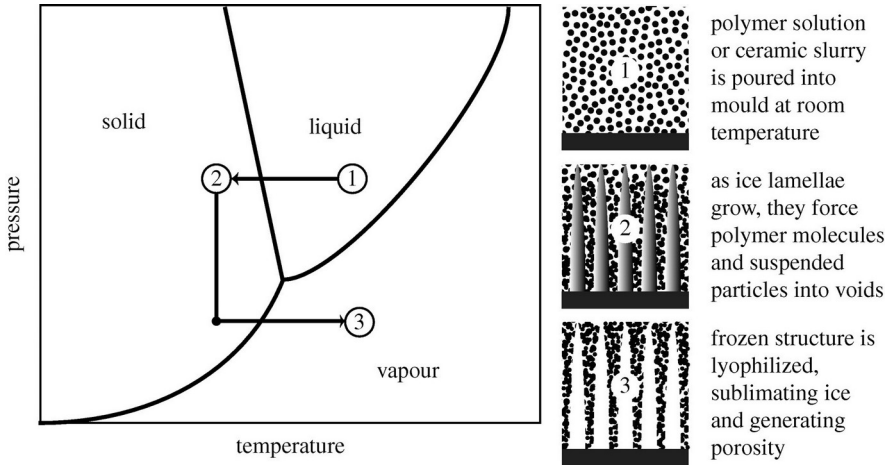

Figure 2. Phase diagram illustrating the phase changes of the liquid vehicle (water here) during the freeze-casting process (Wegst et al., 2010).

2. METHODOLOGY

2.1 Manufacturing and characterization of samples

In order to prepare the samples ceramic slurries were prepared by gradually combining distilled water, alumina powder and dispersant in a magnetic stirrer. Then, this mixture was inserted into an ultrasonic probe (Sonics VC750) at amplitude of 30% for 2 min, in order to promote the total deaggregation of the powder particles. The casings were prepared with different mass fraction proportions of alumina (wt%), as shown in Tab. 1.

For the manufacture of the samples through freeze-casting method, the mixture of ceramics and water was poured in a polyester mold (polyethylene terephthalate -PET) and attached to a cold finger, which promotes sample freezing, as depicted in Fig. 3. In the cold finger, one end of the copper rod is inserted in liquid nitrogen, while the base of the aforementioned PET mold is attached to the other. This setup freezes the slurry starting from the bottom towards the top of the mold, and that causes the ice crystals to form oriented in the freezing direction. The samples manufactured through the process were designed for a final size of about 30 mm in diameter and variable height between 15 and 22 mm.

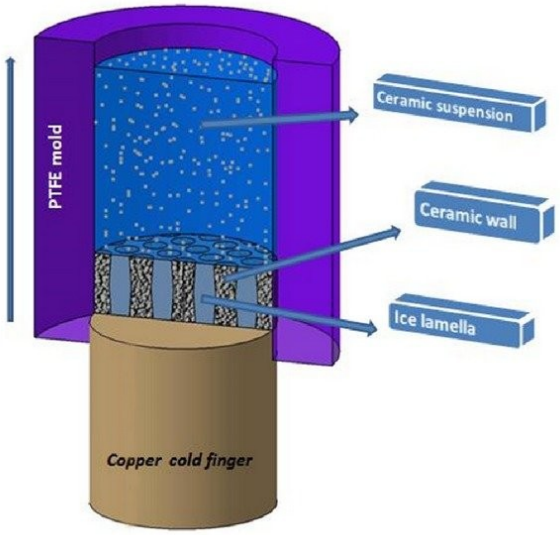

Figure 3. A schematic of freeze casting method (Touri et al., 2013).

After completely frozen, samples were placed in a freezer with a temperature about 193 K during 12 hours and then freeze dried for 48 hours. After lyophilization, the samples were sintered. Sintering was performed in a high temperature oven (EDG1800-S 10P). Heating rate and sintering times were varied as shown in Tab. 1.

Table 1. Sintering conditions.

Groups	Heating rate [°C/min]	Sintering time [h]
A (50 wt%)	10	4
B (50 wt%)	10	8
C (50 wt%)	5	4
D (60 wt%)	10	4
E (65 wt%)	10	4

Sintered ceramic samples were characterized taking into account the porosity (ε), critical diameter (d_c) and permeability (K), as proposed in the following:

$$\varepsilon = \frac{V_p}{V_t} \tag{1}$$

$$\varepsilon = \left(\frac{m_i - m_s}{\rho_{h2o}}\right)\left(\frac{m_i - m_s}{\rho_{h2o}} + \frac{m_s}{\rho_{al2o3}}\right)^{-1} \tag{2}$$

$$d_c = \frac{4\,\sigma \cos\theta}{\Delta P_{cap}} \tag{3}$$

$$K = \frac{\mu \dot{V} L}{\Delta P A} \tag{4}$$

In Eq. (1), V_t is the total sample volume, V_p is the total pore volume. The porosity (ε) was estimated from Eq. (2), where m_i is the mass of the sample immersed in water, m_s is the mass of the dry sample, ρ_{h2o} is the density of water and ρ_{al2o3} is the density of alumina.

The critical diameter (d_c) was estimated from Eq. (3), where σ is the surface tension of water, θ the contact angle of water with solid and dP_{cap} the capillary pressure, which is the difference between the gauge pressure applied on the gas line and the pressure of the water column above the sample. In this paper the contact angle was considered equal to 0°.

Equation (4) represents the permeability from the Darcy's law, where μ is the fluid viscosity, $\dot{V}$ the volumetric flow, L the thickness of the sample, ΔP the pressure drop measured along the sample, and A the cross-sectional area of the sample.

2.2 Thermal performance

A CPL setup available at LabCET was used to assess thermal performances of selected samples from measurements of power inputs and operating temperatures, using deionized water as working fluid.

The experimental apparatus include thermocouples (Omega) T-type and a computer connected to a data acquisition system (Agilent 34970A) for temperature reading. The thermocouples were fixed along the capillary evaporator, condenser, reservoir and the liquid and vapor lines, as shown in Fig. 1. A power source (Agilent N6700B) and electric heaters were used to supply heat loads on the upper surface of the evaporator and also in the reservoir. The condenser was cooled by water using a cryostat bath (Microquímica MQBMP-01) as heat sink. The power input was applied at steps from 5 to 44 watts.

The total thermal resistance, R (K/W), is estimated using the equation

$$R = \frac{T_{evap} - T_{cool}}{Q} \tag{5}$$

where Q (W) is the thermal load, T_{evap} (°C) is the outer surface temperature on the evaporator, and T_{cool} (°C) is the temperature of the cooling water measured at the condenser inlet

The heat flux applied (W/cm²) on the evaporator surface is

$$Q" = \frac{Q}{A_{heat}} \tag{6}$$

where A_{heat} is the heated area. So, it is obtained the thermal resistance (cm²·K/W) that takes into account the heated area,

$$R" = \frac{T_{evap} - T_{cool}}{Q"} \tag{7}$$

The expanded measurement uncertainties were estimated with 95 % confidence interval following recommendations from the Guide to the Expression of Uncertainty in Measurement (ABNT and INMETRO, 2003). The power input uncertainty remained below 0.6 W, while the temperature uncertainty remained below 0.7 °C.

3. RESULTS AND DISCUSSION

3.1 Ceramic characterization

Table 2 shows results concerning sample characterization, which are consistent with results in current technical literature (Berti, 2008; Berti et al., 2008; Choi et al., 2014; Deschamps et al., 2015; Semenic and Catton, 2009; Xu et al., 2013).

Table 2. Characterization results.

Sample groups	ε [%]	K [10^{-12}m²]	d_c [µm]	ΔP_{cap} [kPa]
A (50 wt%)	83.7	5.5 ± 1.2	16,4	16.9 ± 2.5
B (50 wt%)	74.3	4.1 ± 1.2	39.7	7.4 ± 2.5
C (50 wt%)	68.9	1.1 ± 1.2	35.6	8.3 ± 2.5
D (60 wt%)	78.5	5.7 ± 1.2	13.7	21.8 ± 2.5
E (65 wt%)	77.0	3.9 ± 1.2	10.9	26.4 ± 2.5

Figure 4 shows the microstructure of a sintered porous Al_2O_3 ceramic prepared from a suspension with 65 %wt. solid loading from scanning electron microscopy (SEM, Hitachi TM3030). As expected, the porous structure is similar to the solvent structure (water in this case), presenting a lamellar porous structure due to the anisotropic interface kinetics of ice (Deville et al., 2007).

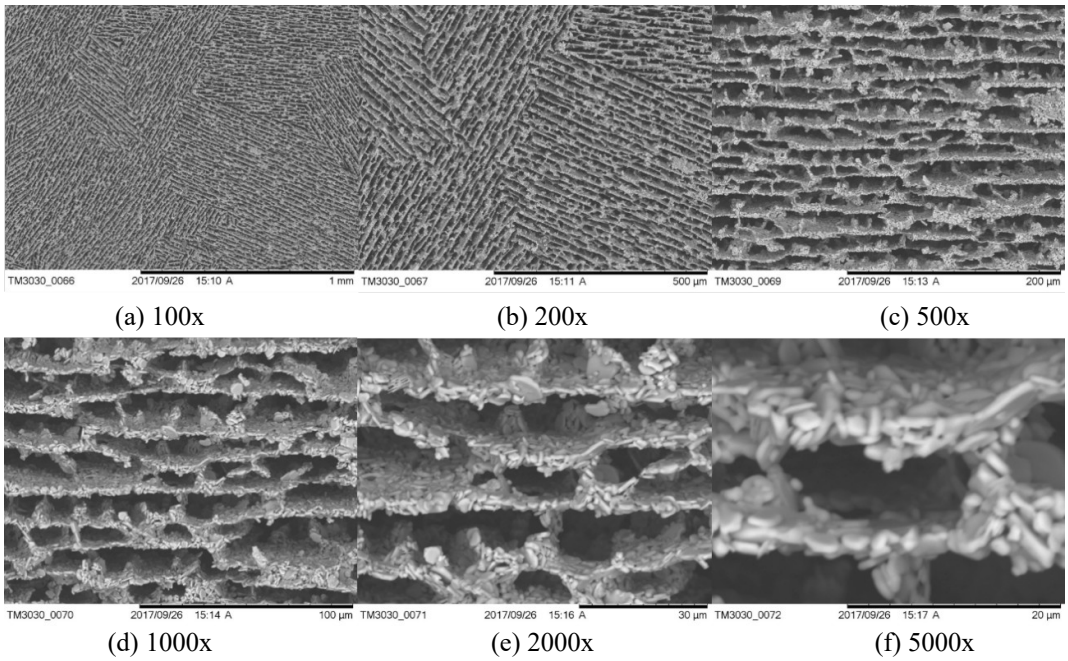

(a) 100x (b) 200x (c) 500x

(d) 1000x (e) 2000x (f) 5000x

Figure 4. SEM transverse cross-section: micro-morphologies of the porous ceramic.

3.2 CPL performance

In this work three samples from group A were selected and assembled in the CPL setup for thermal performance analysis. Figure 5 shows the behavior of the system as the thermal load was increased. The heat sink temperature was set at 15 °C and the room temperature was measured around 23 °C. Despite the evaporator surface temperature reaching inadequate values for some applications, the CPL behaved satisfactorily, remaining stable at thermal load levels from 5 to 35 W. It should be noted there were no observed temperature peaks that usually occur at startup, which are related to the boiling process in the evaporator and displacement of liquid from the vapor channels to the condenser.

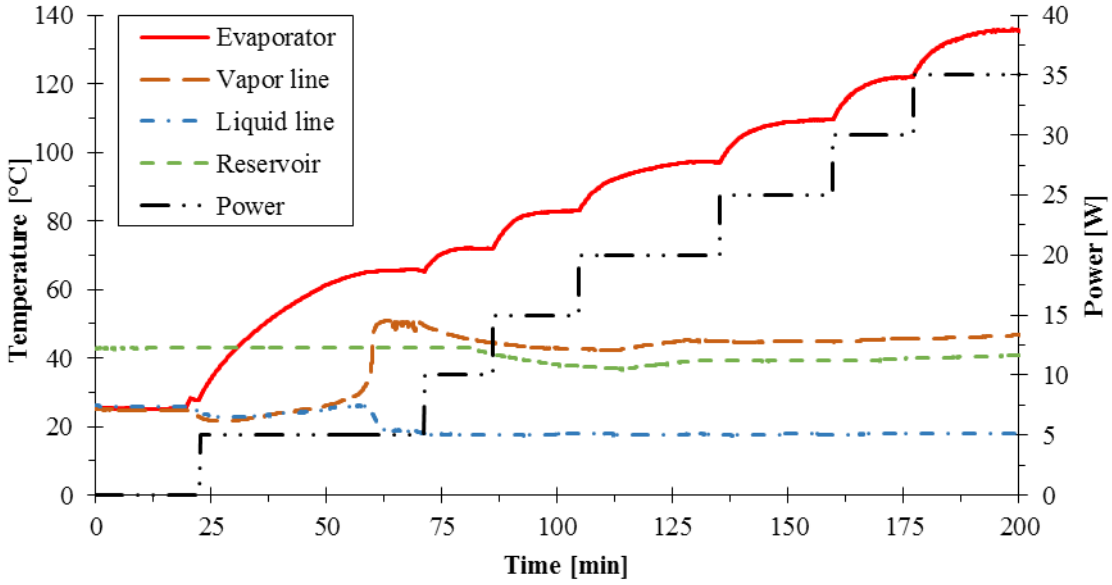

Figure 5. Temperatures of the CPL for heat loads increasing.

As mentioned before, the thermal performance of the system was assessed by the total thermal resistance. Thermal performance tests were carried out with three samples from group A, as shown in Fig. 6. It is observed the same order of magnitude for each thermal load. In addition, there is a trend for thermal resistance decrease to a minimum level of around 3 K /W (16 cm²·K/W) as the applied thermal load increases. It should be noted that the uncertainties associated with the applied power remained below 0.6 W, and in order to avoid graphic pollution, the error bars of the X-axis were omitted from Fig. 6a.

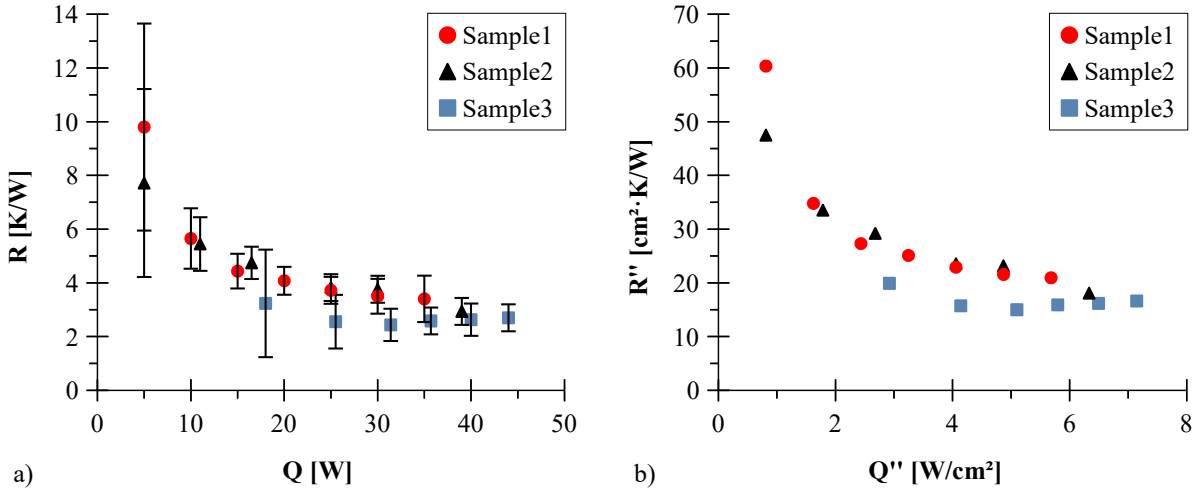

Figure 6. (a) Total thermal resistance vs. total applied power and (b) total thermal resistance per square centimeter vs. heat flux

Some works related to thermal analysis of CPLs were used in an expanded comparison with the present work, as shown in Figs. 7 and 8. The working pairs (capillary structure/working fluid) used in each research were: Odagiri et al. (2020) - stainless steel/acetone; Santos et al. (2012) - ceramic/water; Joung et al. (2010) - stainless steel/water; Lin and Lin (2009) - high density polyethylene/HCFC 141b; Tsujimori et al. t(2008) - teflon/HFC134a; Camargo (2004) - ceramic/water.

Figure 7 presents a comparison of thermal resistances as a function of applied powers. In this case, the results are not very attractive. However, when the heated area is taken into account, a significant improvement can be appreciated, as shown in Fig. 8. On the other hand, by limiting the comparison with the same working pairs of the present work (ceramic/water), it is evident that the new capillary evaporator has superior performance.

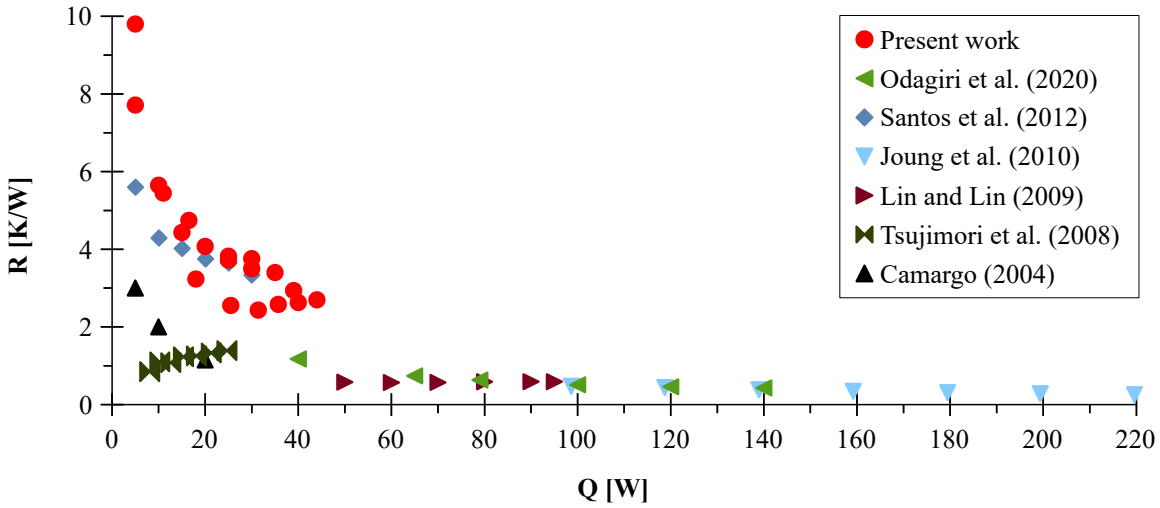

Figure 7. Comparison with the technical literature: thermal resistance vs. applied power.

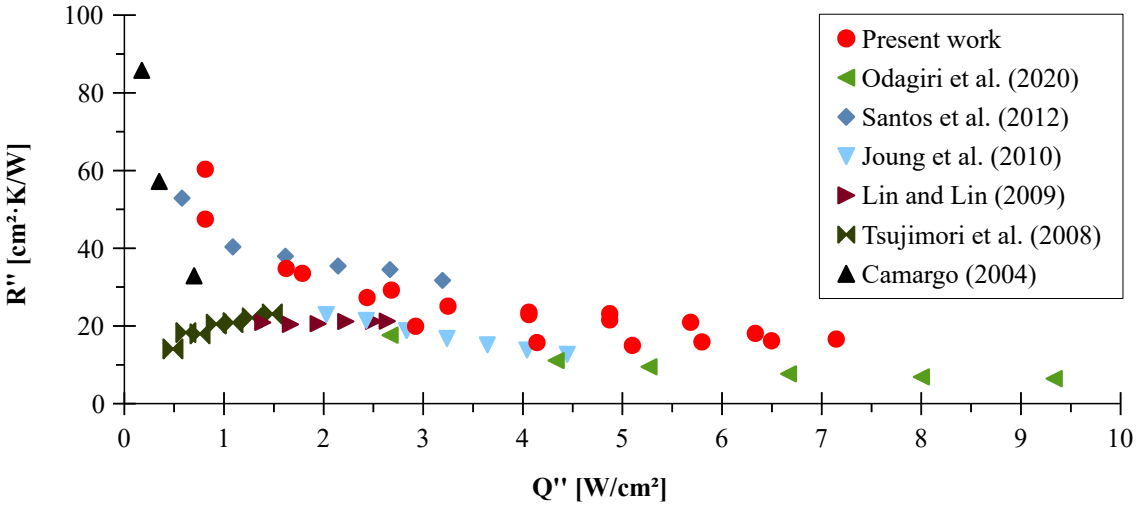

Figure 8. Comparison with the technical literature: thermal resistance per square centimeter vs. heat flux.

The results presented here are still preliminary. Further investigations are necessary, such as manufacturing parameters of the capillary structure, characterization procedures, working fluid inventory and other working fluids.

4. CONCLUSIONS

This work proposes a new method of manufacturing capillary evaporators. Alumina structures were manufacturing from the freeze casting method, characterized and integrated in a CPL to demonstrate the thermal performance obtained from this technology.

From the characterization procedures, the results were consistent with the current technical literature, proving suitable to be integrated in two-phase thermal control systems such as CPLs.

In thermal performance tests, CPL was able to operate stably with powers up to 44 W (7 W/cm²), corresponding to a total thermal resistance of about 3 K/W (16 cm²·K/W), showing promise when compared with similar thermal control systems.

Although further investigations are necessary, the freeze casting method proved to be successful and valid for the manufacture of ceramic capillary evaporators.

5. ACKNOWLEDGMENTS

This work is supported by CNPq as a financial support.

6. REFERENCES

ABNT, INMETRO, 2003. Guide to the expression of uncertainty in measurement (in Portuguese), 3rd ed. ABNT, INMETRO, Rio de Janeiro.

Baumgratz, F.M., Oro, M.V., Fredel, M.C., Bazzo, E., 2017. The freeze casting method as a production alternative for ceramic capillary evaporators, in: 24th ABCM International Congress of Mechanical Engineering. ABCM, Curitiba.

Berti, L.F., 2008. Characterization of ceramic wicks for application in capillary pumping systemss (in portuguese).

Berti, L.F., Rambo, C.R., Reimbrecht, E.G., Bazzo, E., Hotza, D., 2008. Production and characterization of ceramic porous elements for capillary evaporators (in portuguese). Exacta 6, 57–64. https://doi.org/10.5585/exacta.v6i1.812

Berti, L.F., Santos, P.H.D., Bazzo, E., Janssen, R., Hotza, D., Rambo, C.R., 2011. Evaluation of permeability of ceramic wick structures for two phase heat transfer devices. Appl. Therm. Eng. 31, 1076–1081. https://doi.org/10.1016/J.APPLTHERMALENG.2010.12.001

Camargo, H.V.R., 2004. Experimental and theoretical evaluation of porous elements applied to capillary pumping systems (in Portuguese). Federal University of Santa Catarina.

Cerza, M., Herron, R.C., Harper, J.J., 2001. The Effect of Sink Temperature on a Capillary Pumped Loop Employing a Flat Evaporator and Shell and Tube Condenser, in: Proceedings of the ASME 2001 International Mechanical Engineering Congress and Exposition. New York, NY, USA, pp. 1–8. https://doi.org/10.2172/821698

Choi, J., Yuan, Y., Sano, W., Borca-Tasciuc, D.A., 2014. Low temperature sintering of copper biporous wicks with improved maximum capillary pressure. Mater. Lett. 132, 349–352. https://doi.org/10.1016/j.matlet.2014.06.090

Deschamps, I.S., Oro, M. V., Oliveira, M.L., Berti, L.F., Fredel, M.C., Bazzo, E., 2015. Processing and morphological analysis of a two-layer ceramic structure for capillary evaporators, in: In: 23rd International Congress of Mechanical Engineering - COBEM2015. ABCM, Rio de Janeiro.

Deville, S., Saiz, E., Tomsia, A.P., 2007. Ice-templated porous alumina structures. Acta Mater. 55, 1965–1974. https://doi.org/10.1016/j.actamat.2006.11.003

Guo, H., Ji, X., Xu, J., 2020a. Research and development of loop heat pipe - A review. Front. Heat Mass Transf. 14, 1–16. https://doi.org/10.5098/hmt.14.14

Guo, H., Ji, X., Xu, J., 2020b. Enhancement of loop heat pipe heat transfer performance with superhydrophilic porous wick. Int. J. Therm. Sci. 156, 106466. https://doi.org/10.1016/j.ijthermalsci.2020.106466

Hu, Z., Wang, D., Xu, J., Zhang, L., 2020. Development of a loop heat pipe with the 3D printed stainless steel wick in the application of thermal management. Int. J. Heat Mass Transf. 161, 120258. https://doi.org/10.1016/j.ijheatmasstransfer.2020.120258

Joung, W., Hwang, H., Lee, J., 2010. Experimental study on the operating characteristics of a capillary pumped loop with a flat evaporator. Int. J. Heat Mass Transf. 53, 268–275. https://doi.org/10.1016/j.ijheatmasstransfer.2009.09.032

Kumar, N., Arakeri, J.H., 2020. Heat and mass transfer from a system of closely packed capillaries – Possible choice for wicks. Int. J. Therm. Sci. 148, 106151. https://doi.org/10.1016/j.ijthermalsci.2019.106151

Lin, H.W., Lin, W.K., 2009. Thermal analysis of reservoir structure versus capillary pumped loop. Appl. Therm. Eng. 29, 186–194. https://doi.org/10.1016/j.applthermaleng.2008.02.015

Maydanik, Y.F., 2005. Loop heat pipes. Appl. Therm. Eng. 25, 635–657. https://doi.org/https://doi.org/10.1016/j.applthermaleng.2004.07.010

Maydanik, Y.F., Chernysheva, M.A., Pastukhov, V.G., 2014. Review: Loop heat pipes with flat evaporators. Appl. Therm. Eng. https://doi.org/10.1016/j.applthermaleng.2014.03.041

Odagiri, K., Nagano, H., Ogawa, H., 2020. Experimental investigation on thermal characteristics of a capillary pumped loop with different reservoir locations. Int. J. Heat Mass Transf. 158, 119964. https://doi.org/10.1016/j.ijheatmasstransfer.2020.119964

Putra, N., Saleh, R., Septiadi, W.N., Okta, A., Hamid, Z., 2014. Thermal performance of biomaterial wick loop heat pipes with water-base Al2O3 nanofluids. Int. J. Therm. Sci. 76, 128–136. https://doi.org/10.1016/j.ijthermalsci.2013.08.020

Putra, N., Septiadi, W.N., 2017. Improvement of heat pipe performance through integration of a coral biomaterial wick structure into the heat pipe of a CPU cooling system. Heat Mass Transf. und Stoffuebertragung 53, 1163–1174. https://doi.org/10.1007/s00231-016-1890-6

Reimbrecht, E.G., Bazzo, E., Almeida, L.H.S., Silva, H.C., Binder, C., Muzart, J.L.R., 2003. Manufacturing of metallic porous structures to be used in capillary pumping systems. Mater. Res. 6, 481–486. https://doi.org/10.1590/S1516-14392003000400009

Santos, P.H.D., Bazzo, E., Oliveira, A.A.M., 2012. Thermal performance and capillary limit of a ceramic wick applied to LHP and CPL, in: Applied Thermal Engineering. Pergamon, pp. 92–103. https://doi.org/10.1016/j.applthermaleng.2012.02.042

Semenic, T., Catton, I., 2009. Experimental study of biporous wicks for high heat flux applications. Int. J. Heat Mass Transf. 52, 5113–5121. https://doi.org/10.1016/j.ijheatmasstransfer.2009.05.005

Solomon, A.B., Mahto, A.K., Joy, R.C., Rajan, A.A., Jayprakash, D.A., Dixit, A., Sahay, A., 2020. Application of bio-wick in compact loop heat pipe. Appl. Therm. Eng. 169, 114927. https://doi.org/10.1016/j.applthermaleng.2020.114927

Touri, R., Moztarzadeh, F., Sadeghian, Z., Bizari, D., Tahriri, M., Mozafari, M., 2013. The Use of Carbon Nanotubes to Reinforce 45S5 Bioglass-Based Scaffolds for Tissue Engineering Applications. Biomed Res. Int. 2013, 465086. https://doi.org/10.1155/2013/465086

Tsujimori, A., Hirata, K., Nakaguchi, K., Uchida, M., 2008. Heat transport characteristics of capillary pumped loop with plate-type evaporator, in: 2008 11th IEEE Intersociety Conference on Thermal and Thermomechanical Phenomena in Electronic Systems, I-THERM. pp. 12–18. https://doi.org/10.1109/ITHERM.2008.4544247

Wegst, U.G.K., Schecter, M., Donius, A.E., Hunger, P.M., 2010. Biomaterials by freeze casting. Phil. Trans. R. Soc. A. 2099–2121. https://doi.org/10.1098/rsta.2010.0014

Xu, J., Zou, Y., Yang, D., Fan, M., 2013. Development of biporous Ti3AlC2 ceramic wicks for loop heat pipe. Mater. Lett. 91, 121–124. https://doi.org/10.1016/j.matlet.2012.09.083

7. RESPONSIBILITY NOTICE

The authors are the only responsible for the printed material included in this paper.